RESEARCH ARTICLE • OPEN ACCESS

Mathematical Modeling and Parameter Estimation of Meningitis Transmission Dynamic using Vaccination Strategies in Indonesia

Aufa Al Musyarof, Faris Nur Hibban, Mardlijah, and Didik Khusnul Arif

JAMBURA JOURNAL OF MATHEMATICS

Volume 8, Issue 2, Pages 227–234, August 2026

Received 12 June 2026, Revised 3 August 2026, Accepted 6 August 2026, Published 16 August 2026

To Cite this Article : A. A. Musyarof, F. N. Hibban, M. Mardlijah, and D. K. Arif,"Mathematical Modeling and Parameter Estimation of Meningitis Transmission Dynamic using Vaccination Strategies in Indonesia", *Jambura J. Math*, vol. 8, no. 2, pp. 227–234, 2026, *https://doi.org/10.37905/jjom.v8i2.39751*

JOURNAL INFO • JAMBURA JOURNAL OF MATHEMATICS

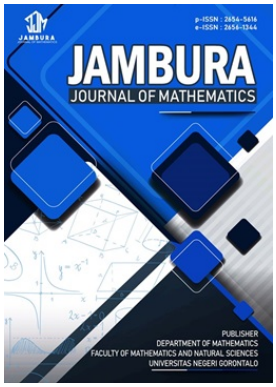

Homepage	:	http://ejurnal.ung.ac.id/index.php/jjom/index
Journal Abbreviation	:	Jambura J. Math.
Frequency	:	Biannual (February and August)
Publication Language	:	English (preferable), Indonesia
DOI	:	https://doi.org/10.37905/jjom
Online ISSN	:	2656-1344
Editor-in-Chief	:	Hasan S. Panigoro
Publisher	:	Department of Mathematics, Universitas Negeri Gorontalo
Country	:	Indonesia
OAI Address	:	http://ejurnal.ung.ac.id/index.php/jjom/oai
Google Scholar ID	:	iWLjgaUAAAAJ
Email	:	info.jjom@ung.ac.id

JAMBURA JOURNAL • FIND OUR OTHER JOURNALS

Jambura Journal of Biomathematics

Jambura Journal of Mathematics Education

Jambura Journal of Probability and Statistics

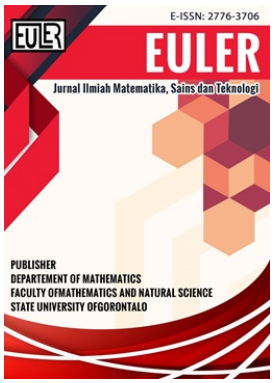

EULER : Jurnal Ilmiah Matematika, Sains, dan Teknologi

Jambura Journal of Mathematics, Volume 8, Issue 2, Pages 227–234, August 2026 https://doi.org/10.37905/jjom.v8i2.39751

Research Article

Check for updates

Mathematical Modeling and Parameter Estimation of Meningitis Transmission Dynamic using Vaccination Strategies in Indonesia

Aufa Al Musyarof[1], **Faris Nur Hibban**[1], **Mardlijah**[1], **Didik Khusnul Arif**[1,*]

[1]*Department of Mathematics, Institut Teknologi Sepuluh Nopember, Surabaya, 60111, Indonesia*

ARTICLE HISTORY
Received 12 June 2026
Revised 3 August 2026
Accepted 6 August 2026
Published 16 August 2026

KEYWORDS
Mathematical modeling
Meningitis dynamics
Parameter Estimation
Sensitivity analysis
Vaccination strategies
Good Health and Well-being

ABSTRACT. *Meningitis is a public health threat because it progresses rapidly and has serious clinical impacts, including long-term disability. This research develops a six-compartment mathematical model to examine the dynamics of meningitis transmission by dividing the population into susceptible, exposed, infected, recovered without disability, recovered with disability, and vaccinated groups. The model parameters were fitted using the least squares method based on annual meningitis case data in Indonesia from 1990 to 2023 according to estimates originating from the Institute for Health Metrics and Evaluation (IHME)/Global Burden of Disease, accessed through the archived Our World in Data source. Model validation shows high accuracy performance, with a Mean Absolute Percentage Error value of 3.12%. Local sensitivity analysis indicates that the transmission rate (β) and vaccination rate (ξ) are the parameters most influencing changes in $\mathcal{R}_0$ resulting from parameter variation. Numerical simulation results show that rapid immunization at the onset of an outbreak is the most effective strategy among the vaccination scenarios examined to expedite herd immunity and limit disease spread.*

1. Introduction

Meningitis remains a significant public health challenge because of its dangerous consequences; even those who have recovered from the disease may experience serious long-term complications [1, 2]. Bacteria, viruses, fungi, and parasites are some of the pathogens that cause meningitis [3–5]. Understanding the dynamics of meningitis transmission is essential for the public so they can prepare in the event of an outbreak in a particular area. This becomes a challenge for Indonesia because the quality of data, such as data accuracy and timeliness of case reporting, is sometimes still delayed, resulting in an increased risk of disease spread [6, 7]. Based on this, an analysis of the dynamics of meningitis transmission can help prevent outbreaks and inform the development of disease control strategies [8, 9].

Previous studies have examined the transmission dynamics of meningitis using various intervention strategies, such as treatment, vaccination, and stability analysis and simulation [10–15]. Research findings from these studies have enhanced our comprehension of how transmission dynamics are influenced by different strategies, allowing for further development or modification of these approaches. As with meningitis itself, individuals who recover from meningitis still face the potential for serious issues such as long-term disabilities [1, 16]. This can be analyzed by distinguishing between individuals who recover without disabilities and those with disabilities. In addition, data calibration using models has not yet been widely integrated into disease spread dynamics modeling; for example, determining appropriate parameter values that align the data with the model also improves the model's ability to accurately depict real-world conditions [17–19].

Based on this, this study developed a data-driven nonlinear model of meningitis transmission dynamics in Indonesia. The population is categorized into six groups: susceptible (S), exposed (E), infected (I), recovered without disability (R_s), recovered with disability (R_d), and vaccinated (V). This model incorporates vaccination strategies, waning vaccine-induced immunity (assuming the vaccine is not perfect), and the effects of treatment on infected individuals, thereby providing a more detailed representation of disease progression and post-infection outcomes, namely recovery without disability and recovery with disability [11, 16].

The analysis of meningitis transmission dynamics in this study was conducted based on annual incidence data for meningitis cases in Indonesia from 1990 to 2023. These estimates originate from the Institute for Health Metrics and Evaluation (IHME)/Global Burden of Disease and were accessed through the archived Our World in Data source [20]. For the purposes of model fitting, these annual incidence data are explicitly treated as a proxy for the infected population compartment (I). The values of the parameters used in this study were estimated using the least squares method. The estimated parameters are expected to calibrate the observed data with the model, thereby representing the dynamics of meningitis transmission [21–23].

The objectives of this study are to formulate the proposed meningitis transmission model, determine the disease-free and endemic equilibrium points, derive the basic reproduction number, and examine the local stability of the disease-free equilib-

*Corresponding Author.

Email : *didik@its.ac.id* (D. K. Arif)
Homepage : http://ejurnal.ung.ac.id/index.php/jjom/index / E-ISSN : 2656-1344

rium. In addition, this study performs parameter estimation, model validation, sensitivity analysis, and numerical simulations to identify the parameters exerting the greatest influence on disease transmission and to evaluate vaccination-related intervention scenarios in Indonesia. By combining a refined epidemiological structure with empirical calibration, this study provides a data-driven framework for analysing meningitis transmission dynamics and vaccination strategies in Indonesia.

2. Method

This research employs mathematical modeling and computational simulation to examine meningitis transmission dynamics and vaccination strategies in Indonesia. The study is based on a nonlinear compartmental epidemiological model that divides the population into six compartments: susceptible (S), exposed (E), infected (I), recovered without disability (R_s), recovered with disability (R_d), and vaccinated (V). This framework explicitly integrates vaccination dynamics, waning immunity, and diverse recovery outcomes into a system of nonlinear differential equations.

Following the model formulation, we analyzed the equilibrium points and system stability to elucidate disease behavior. To ensure the model aligns with observed empirical data, parameter estimation was conducted using the least-squares method based on longitudinal meningitis case records in Indonesia. A local sensitivity analysis was then performed to ascertain the most influential parameters affecting disease transmission. Finally, numerical simulations were employed to investigate various hypothetical vaccination scenarios and their effects on meningitis dynamics. The overall mathematical and computational procedures are summarized in the accompanying flowchart:

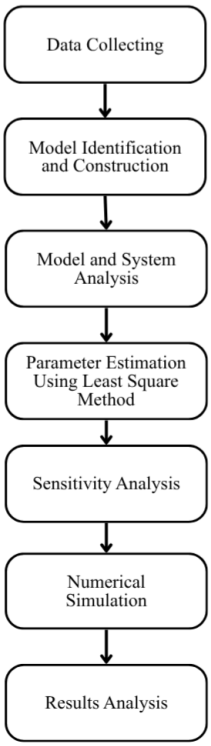

Figure 1. Research method.

3. Results and Discussion

3.1. Mathematical Modeling of Meningitis Transmission Dynamics

The mathematical model is constructed to explain how the disease spreads in a population by categorizing individuals into distinct epidemiological compartments. The model assumes the population is divided into compartments: susceptible, exposed, infected, recovered without disability, recovered with disability, and vaccinated individuals. Newborns enter the susceptible class at a recruitment rate (Λ) as they possess no immunity. Each compartment experiences natural mortality at rate (μ). Susceptible individuals (S) can become exposed (E) through close contact with infected individuals (I). Exposed individuals then undergo an incubation period before transitioning to the infected (I) class at a rate of (σ), during which recovery does not occur. Infected individuals leave the infected compartment through recovery at a per capita rate γ. The dimensionless parameter ε represents treatment effectiveness and is interpreted as the proportion of infected individuals who recover without disability. Therefore, the recovery flow to the recovered-without-disability compartment R_s is given by $\gamma\varepsilon I$, whereas the recovery flow to the recovered-with-disability compartment R_d is given by $\gamma(1-\varepsilon)I$. Furthermore, infection-related mortality occurs at a baseline per capita rate δ. In this model, treatment effectiveness is also assumed to reduce meningitis-related mortality. Thus, the effective disease-induced mortality rate is $\delta(1-\varepsilon)$, yielding the mortality term $\delta(1-\varepsilon)I$.

Based on the above assumptions, a compartment diagram can be drawn on Figure 2. This framework provides a comprehensive representation of disease progression and control measures, enabling the analysis of vaccination and treatment effects on disease outcomes.

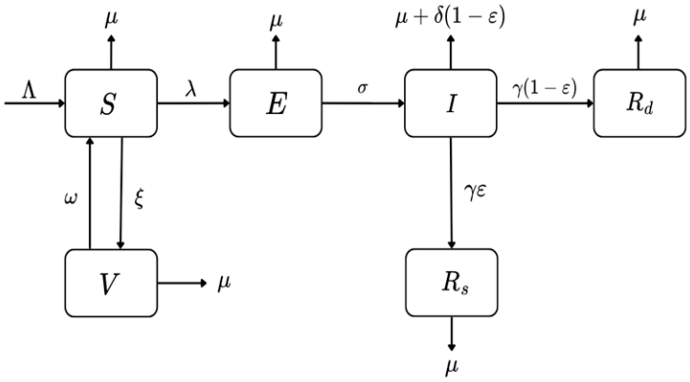

Figure 2. Compartment diagram of meningitis mathematical model.

The force of infection is defined as $\lambda = \beta I/N$, which represents the per capita rate at which a susceptible individual acquires infection and enters the exposed compartment through contact with infectious individuals. Therefore, the incidence term for new exposures is given by $\lambda S = \beta SI/N$. This incidence term appears as a loss term in the susceptible equation and as a gain term in the exposed equation. The total population is defined as $N = S + E + I + R_s + R_d + V$. Table 1 provides detailed descriptions of the model parameters.

The construction of a mathematical model to describe meningitis spreads is represented by a system of nonlinear dif-

Table 1. Model parameters, definitions, units, and sources.

Parameter	Definition	Unit	Values
Λ	Recruitment rate	People per year	Calculated from demographic data
μ	Natural death rate	Per year	Calculated from demographic data
β	Transmission rate	Per year	Model-fitted
σ	Rate of transition of individuals	Per year	Model-fitted
γ	Recovery rate	Per year	Model-fitted
δ	Meningitis death rate	Per year	Model-fitted
ξ	Vaccination rate	Per year	Model-fitted
ω	Vaccine immunity decline rate	Per year	Model-fitted
ε	Treatment effectiveness	Nondimensional	Model-fitted

ferential equations as follows:

$$\frac{dS}{dt} = \Lambda - \frac{\beta SI}{N} + \omega V - (\mu + \xi)S, \tag{1}$$

$$\frac{dE}{dt} = \frac{\beta SI}{N} - (\mu + \sigma)E, \tag{2}$$

$$\frac{dI}{dt} = \sigma E - (\mu + \delta(1-\varepsilon))I - \gamma I, \tag{3}$$

$$\frac{dR_s}{dt} = \gamma\varepsilon I - \mu R_s, \tag{4}$$

$$\frac{dR_d}{dt} = \gamma(1-\varepsilon)I - \mu R_d, \tag{5}$$

$$\frac{dV}{dt} = \xi S - (\mu + \omega)V. \tag{6}$$

3.2. Disease-Free equilibrium

In mathematical epidemiology, two principal equilibrium points are commonly considered: the disease-free equilibrium, characterized by the absence of disease in the population, and the endemic equilibrium, in which the disease persists in the population. These equilibrium points are determined by setting the right-hand sides of eq. (1)–(6) equal to zero. The disease-free equilibrium is obtained by setting the infection-related state variables equal to zero, that is, $E = I = 0$. Solving the resulting algebraic system yields the following disease-free equilibrium:

$$(S_0^*, E_0^*, I_0^*, R_{s,0}^*, R_{d,0}^*, V_0^*) = \left(\frac{\Lambda(\mu+\omega)}{\mu(\mu+\omega+\xi)}, 0, 0, 0, 0, \frac{\Lambda\xi}{\mu(\mu+\omega+\xi)}\right). \tag{7}$$

3.3. Basic Reproduction Number

Epidemiologically, the R_0 value obtained from this modeling serves as the main threshold parameter that controls the entire long-term dynamics of disease spread. If medical intervention succeeds in suppressing this parameter value until $R_0 < 1$, then the disease-free equilibrium point is mathematically proven to be locally asymptotically stable, indicating that the chain of transmission will be broken and the disease will disappear from the population over time. Conversely, if $R_0 > 1$, the disease will persistently invade the population and lead to endemic conditions [11].

The Next Generation Matrix (NGM) method separates the new infection terms represented by the matrix F from other transitions among the infected compartments represented by the matrix V. The spectral radius of the next-generation matrix FV^{-1} represents the expected number of secondary infections generated by a single infected individual during its infectious period [10]. The basic reproduction number is determined using the NGM method through the following steps:

1. Linearize the infected subsystem around the disease-free equilibrium point. This linear system is represented by the Jacobian matrix (J):

$$J(E_0^*, I_0^*) = \begin{bmatrix} -(\mu+\sigma) & \dfrac{\beta S}{N} \\ \sigma & -(\mu+\delta(1-\varepsilon)+\gamma) \end{bmatrix}.$$

2. Decompose the Jacobian matrix (J) into the transmission matrix (F) and the transition matrix (V), $J = F - V$. The transmission matrix is a matrix with entries that represent the occurrence of new infections, while the transition matrix is a matrix with entries that represent changes in the infected population:

$$\mathcal{F} = \begin{bmatrix} 0 & a \\ 0 & 0 \end{bmatrix}, \quad \mathcal{V} = \begin{bmatrix} b & 0 \\ -\sigma & c \end{bmatrix}, \quad \mathcal{V}^{-1} = \begin{bmatrix} \dfrac{1}{b} & 0 \\ \dfrac{\sigma}{bc} & \dfrac{1}{c} \end{bmatrix},$$

where

$$a = \frac{\beta(\mu+\omega)}{\mu+\omega+\xi}, \quad b = \sigma + \mu, \quad c = \mu + \delta(1-\varepsilon) + \gamma.$$

3. The basic reproduction number is defined as $R_0 = \rho\left(\mathcal{F}\mathcal{V}^{-1}\right)$, where ρ denotes the spectral radius of a matrix. Therefore, for the proposed model, the basic reproduction number is given by

$$\mathcal{R}_0 = \frac{\sigma\beta(\mu+\omega)}{(\mu+\omega+\xi)(\mu+\sigma)(\mu+\delta(1-\varepsilon)+\gamma)}. \tag{8}$$

3.4. Endemic equilibrium point

The endemic equilibrium point represents a positive steady-state solution, indicating the disease's persistence within the observed population. This point is determined by setting each equation in the model, as shown in Eq. (1)–(6), to zero. Consequently, the endemic equilibrium point is expressed as follows:

$$S_1^* = \frac{\Lambda(\mu+\omega)(\delta\mu+\gamma\mu+\gamma\sigma+\mu\sigma+\mu^2-\delta\epsilon\mu)}{\mu(\mu+\omega+\xi)\Phi},$$

$$I_1^* = \frac{\Lambda\sigma(R_0-1)}{\Phi},$$

$$E_1^* = \frac{\Lambda(R_0-1)(\delta+\gamma+\mu-\delta\varepsilon)}{\Phi},$$

$$R^*_{s,1} = \frac{\Lambda\varepsilon\gamma\sigma(R_0-1)}{\mu\Phi},;$$
$$V^*_1 = \frac{\Lambda\xi(\delta\mu+\gamma\mu+\gamma\sigma+\mu\sigma+\mu^2-\delta\varepsilon\mu)}{\mu(\mu+\omega+\xi)\Phi},$$
$$R^*_{d,1} = \frac{-\Lambda\gamma\sigma(R_0-1)(\varepsilon-1)}{\mu\Phi},$$

where

$$\Phi = \mathcal{R}_0\mu^2 - \delta\sigma + \mathcal{R}_0\delta\mu + \mathcal{R}_0\gamma\mu + \mathcal{R}_0\delta\sigma + \mathcal{R}_0\gamma\sigma + \mathcal{R}_0\mu\sigma + \delta\varepsilon\sigma - \mathcal{R}_0\delta\varepsilon\mu - \mathcal{R}_0\delta\varepsilon\sigma.$$

3.5. Parameter Estimation

The annual incidence estimates used in this study originate from the Institute for Health Metrics and Evaluation (IHME)/Global Burden of Disease and were accessed through the archived Our World in Data source. The data collected was the number of meningitis cases in Indonesia in the period 1990-2023. This section presents the calculation of the parameter values used in the model. The parameters are computed based on assumptions and the available data, with the rate of change of the parameter values assumed to remain constant over time. The following details are the calculation of the parameters for the meningitis transmission model:

1. Recruitment rate (Λ)
   The recruitment rate is the constant rate of addition of new individuals to a susceptible population (S) per unit time. It is assumed that all new individuals are born susceptible. The recruitment rate is often calculated based on the total population size and crude birth rate (CBR). The CBR in Indonesia is 16.4 births per 1,000 population [24]. The total population in Indonesia in 2026 is 288,315,089 [25]. So that the recruitment rate is obtained:
   $$\Lambda = 0.0164 \cdot 288,315,089 \approx 4,728,367.$$
2. Natural death rate (μ)
   In epidemiological models, the natural mortality rate is directly associated with the population's life expectancy. The calculation of the natural death rate based on data in Indonesia is as follows [26]:
   $$\mu = \frac{1}{\text{Life expectancy}} = \frac{1}{74.47} = 0.0134.$$

The initial values of the variables were derived from demographic and epidemiological data in Indonesia for the year 1990. The susceptible population (S) was based on the total population of Indonesia in 1990, which numbered 179,378,946 [27]. The number of infected individuals (I) was obtained from reported meningitis cases in Indonesia during the same year, amounting to 168,257. Because empirical initial values for the remaining compartments were unavailable in the public datasets, the assumptions of $E(0) = R_s(0) = R_d(0) = V(0) = 0$ were utilized. Therefore, the exposed population (E), recovered with disability (R_d), recovered without disability (R_s), and vaccinated individuals (V) were all initially set to zero.

3.6. Parameter Fitting Using Least Square Method

Using least squares estimation via the `least_squares` function from the SciPy library in Python, the nonlinear compartmental model proposed in eqs. (1)–(6) was adapted to annual meningitis case incidence data in Indonesia from 1990 to 2023. The optimization utilized the Trust Region Reflective (TRF) algorithm, which is highly suited for bounded parameter fitting. During the fitting process, the ordinary differential equations (ODE) were solved using the Radau method, an implicit Runge-Kutta solver known for its stability. The initial guesses for the parameters $[\Lambda, \mu, \beta, \sigma, \gamma, \delta, \xi, \omega, \varepsilon]$ were set to [4,728,367.0, 0.0133, 0.3, 0.2, 0.2, 0.1, 0.1, 0.1, 0.5]. The search space was constrained with lower bounds of [4,728,366.0, 0.0132, 0.01, 0.01, 0.01, 0.01, 0.01, 0.01, 0.01] and upper bounds of [4,728,368.0, 0.0134, 2.0, 1.0, 1.0, 1.0, 1.0, 1.0, 1.0]. Furthermore, default algorithm settings were employed for the stopping tolerances (with a function tolerance of 10^{-8}) and a maximum limit of function evaluations to ensure convergence. This fitting process focused on visualizing long-term downward trends and reported annual fluctuations to extract realistic and data-driven parameter estimates. Empirical data originating from the IHME/Global Burden of Disease exclusively provides the annual incidence of clinically reported cases. Consequently, these annual incidence data are explicitly treated as a proxy for the infected population compartment (I) for the purposes of model fitting.

Conversely, the available public Indonesian datasets lack direct empirical observations for the exposed population (E), individuals who recovered without disability (R_s), those who recovered with disability (R_d), and vaccinated individuals (V). As a result, these unobserved compartments were mathematically reconstructed using the model's internal dynamic structure, incorporating parameter values from existing literature and adjusted initial conditions. This methodology aligns with previous studies on meningitis modeling, where only temporal data on the infected population was accessible. The states of the other compartments were inferred through model simulations. Mathematical models were thus developed to interpret the unobserved system from observed data, facilitating parameter estimation and scenario analysis despite incomplete data [28].

3.7. Model Fitting Evaluation

After parameter estimation was conducted and the results were obtained, model validation was subsequently performed to determine the appropriate variables by substituting the estimated parameters and the initial values of the variables into the discrete system model. The best parameter values obtained from the estimation are presented in the Table 2.

Table 2. Parameter estimation results.

Parameter	Definition	Values
Λ	Recruitment rate	4,728,367
μ	Natural death rate	0.0134
β	Transmission rate	0.067713
σ	Rate of transition of individuals	0.999995
γ	Recovery rate	0.046768
δ	Meningitis death rate	0.033465
ξ	Vaccination rate	0.111910
ω	Vaccine immunity decline rate	0.010344
ε	Treatment effectiveness	0.834280

These parameters were used for model validation, as shown in Figure 3. To evaluate the performance of these esti-

mated parameters, an assessment was conducted. Given that the obtained value is well below the 10% threshold, the fitted model shows close agreement with the observed annual data, with a MAPE of 3.12%.

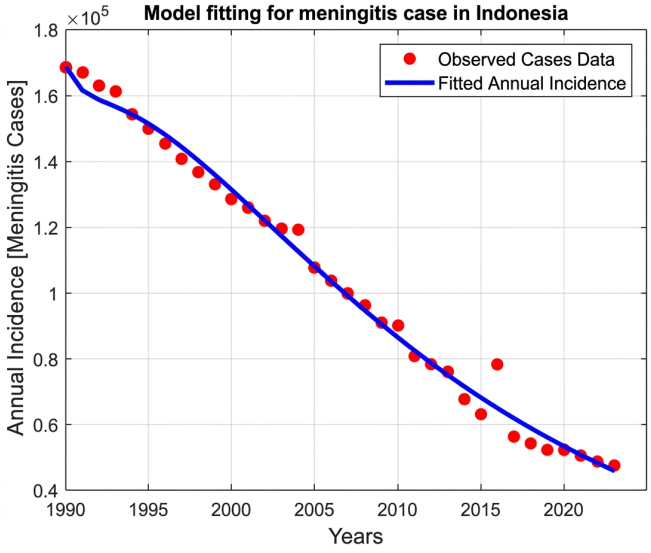

Figure 3. Validation of the model using infected data.

3.8. Stability Analysis

The mathematical model of the spread of meningitis in eq. (1)–(6) is a nonlinear differential system. Therefore, before carrying out stability analysis, it is necessary to carry out linearization. Linearization of the system can be done through Taylor expansion around the equilibrium point. Linearization around the disease-free equilibrium point with Jacobian matrix i.e.

$$J = \begin{bmatrix} j_{11} & 0 & j_{13} & 0 & 0 & \omega \\ 0 & j_{22} & j_{23} & 0 & 0 & 0 \\ 0 & \sigma & j_{33} & 0 & 0 & 0 \\ 0 & 0 & \gamma\varepsilon & -\mu & 0 & 0 \\ 0 & 0 & \gamma(1-\varepsilon) & 0 & -\mu & 0 \\ \xi & 0 & 0 & 0 & 0 & -(\mu+\omega) \end{bmatrix}, \quad (9)$$

where

$$j_{11} = -(\mu+\xi), \quad j_{13} = -\frac{\beta(\mu+\omega)}{\mu+\omega+\xi},$$
$$j_{22} - (\mu+\sigma), \quad j_{23} = \frac{\beta(\mu+\omega)}{\mu+\omega+\xi},$$
$$j_{33} = -(\mu+\delta(1-\varepsilon)+\gamma).$$

The stability analysis of the disease-free equilibrium point was carried out by substituting the parameter values given in Table 2 into the Jacobian matrix obtained in eq. (9), as follows:

$$J = \begin{bmatrix} -0.1253 & 0 & -0.0119 & 0 & 0 & 0.0103 \\ 0 & -1.0134 & 0.0119 & 0 & 0 & 0 \\ 0 & 0.9999 & -0.0657 & 0 & 0 & 0 \\ 0 & 0 & 0.0390 & -0.0134 & 0 & 0 \\ 0 & 0 & 0.0078 & 0 & -0.0134 & 0 \\ 0.1119 & 0 & 0 & 0 & 0 & -0.0237 \end{bmatrix}$$

Thus, the eigenvalues are $\lambda_1 = -0.013400$, $\lambda_2 = -0.013400$, $\lambda_3 = -1.025740$, $\lambda_4 = -0.135654$, $\lambda_5 = -0.053368$, $\lambda_6 = -0.013400$. For the estimated parameter values, all eigenvalues have negative real parts, indicating local asymptotic stability of the disease-free equilibrium.

3.9. Sensitivity Analysis

The sensitivity analysis conducted in this research is a local sensitivity analysis. The normalized sensitivity index of variable X, differentiable on parameter p, is defined as follows:

$$C_p^X = \frac{\partial X}{\partial p} \times \frac{p}{X}.$$

where X is the variable to be analyzed and p is the parameter. The higher the sensitivity index value, the more influential the parameter is. Positive and negative signs indicate the relationship between the parameter and the variables being analyzed, namely the basic reproduction number and the infection set point.

This section will analyze the sensitivity of parameters to the basic reproduction number. A sensitivity analysis of R_0 was conducted to determine which parameters exert the most significant influence on R_0. Based on the parameter values in Table 2, the basic reproduction number value is $R_0 = 0.1778$. The sensitivity index of the parameter σ is:

$$C_\sigma^{\mathcal{R}_0} = \frac{\partial \mathcal{R}_0}{\partial \sigma} \times \frac{\sigma}{\mathcal{R}_0} = \frac{\mu}{\mu+\sigma}.$$

Using the same procedure, sensitivity index for other parameters were obtained. The parameter values in Table 2 are used to calculate the sensitivity index value. To evaluate the consistency of the relationship between the parameter and the basic reproduction number, the parameter value was increased and decreased by 10%, and the resulting variations in the basic reproduction number were analyzed.

Table 3. Parameter sensitivity of the basic reproduction number.

Parameter	Sensitivity Index	$\mathcal{R}_0$: $p-10\%$	$\mathcal{R}_0$: $p+10\%$
μ	0.2486	0.1732	0.1821
β	1	0.1600	0.1956
σ	0.0132	0.1775	0.1780
γ	-0.7110	0.1914	0.1660
δ	-0.0852	0.1793	0.1763
ξ	-0.8250	0.1938	0.1643
ω	0.3594	0.1714	0.1842
ε	0.4236	0.1706	0.1857

The sensitivity index results indicate that the most influential parameters to $\mathcal{R}_0$ are the transmission rate (β) and the vaccination rate (ξ). Specifically, based on the absolute sensitivity values, β has the largest positive influence, while ξ has the largest negative influence on $\mathcal{R}_0$. To test whether the relationship between the parameters and the basic reproduction number is consistent, a 10% increase or decrease in the parameter value is applied to observe changes in the basic reproduction number. Increasing the parameter β by 10% increases the $\mathcal{R}_0$ value from 0.1778 to 0.1956. Conversely, decreasing the parameter β by 10% also decreases the $\mathcal{R}_0$ value. This demonstrates that the analysis results are consistent with the experimental results on the $\mathcal{R}_0$ value.

3.10. Numerical Simulation

In this section, numerical simulations are carried out to analyse in depth the dynamics of the meningitis transmission model in Indonesia based on the system of nonlinear differential in eq. (1)–(6). The simulations were run using MATLAB software to observe population trajectory behaviour over the period from 1990 to 2023, corresponding directly to the time range of the available actual empirical data. The initial conditions of the system are strictly defined based on 1990 demographic data, $S(0) = 179,378,946$ and $I(0) = 168,257$, whilst the other state variables are initialised to zero.

Based on the results of the sensitivity analysis in the previous subsection, the transmission rate β and the vaccination rate ξ were identified as the two main parameters exerting the most dominant control over changes in the basic reproduction number $\mathcal{R}_0$ resulting from parameter variation. Therefore, the simulation focused on two hypothetical intervention scenarios to examine the sensitivity of the response of the susceptible population S to changes in transmission rates, as well as the vaccinated population V to strengthening the immunization program.

The parameter β measures the intensity of meningitis transmission within a population. To thoroughly evaluate the system's resilience under extreme conditions—such as a sudden severe outbreak or a massive expansion of social contacts—we simulated scenarios using significantly elevated transmission rates. Because the selected values of $\beta = 0.3, 0.5, 0.8$, and 1 are substantially larger than the estimated baseline value of $\beta = 0.067713$, they serve as hypothetical high-transmission scenarios designed to illustrate worst-case epidemic dynamics. Thus, the simulation is divided into five levels: the estimated baseline $\beta = 0.067713$, alongside the hypothetical values $\beta = 0.3$, $\beta = 0.5$, $\beta = 0.8$, and $\beta = 1$. The results of the simulation of the susceptible population (S) are presented in Figure 4.

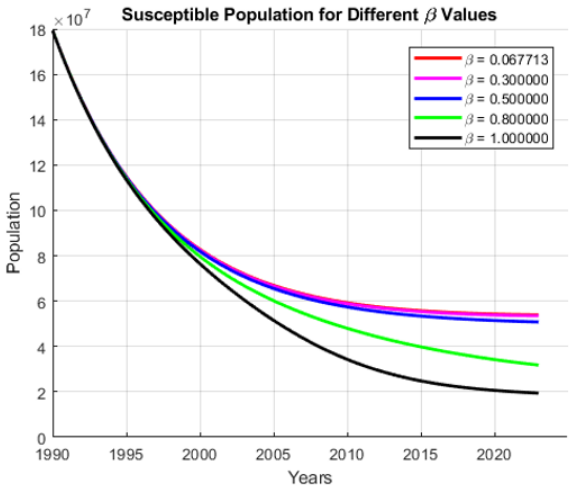

Figure 4. Dynamics of the susceptible population to the transmission rate.

The simulation results in Figure 4 show that at a value of $\beta = 0.067713$, the susceptible population curve flattens gradually towards a figure approaching $5,4 \times 10^7$ individuals by 2023. An interesting phenomenon occurs when the value of β is increased aggressively. Theoretically, an increase in the transmission rate triggers a much faster depletion of the susceptible population due to the high rate of conversion from susceptible individuals to exposed individuals.

However, the graph results show that when β increased from 0.3 to 0.5, the curves of the susceptible population decline overlap closely, and the most extreme level of susceptible population depletion occurs exponentially in the maximum transmission scenario, $\beta = 1$. This indicates a rapid depletion of the susceptible population under very high transmission rates in the short-term modeling, 33 years. When infections spread very rapidly, the initial limitation on the number of susceptible individuals causes the S curve to plummet drastically until it reaches a critical level of approximately 1.9×10^7 individuals by the end of the observation period.

Parameter ξ represents the government's preventive intervention in moving vulnerable individuals into the protected compartment V. Through this scenario analysis, we simulate the impact of strengthening immunization coverage policy from the actual fitted value $\xi = 0.111910$ towards more extensive scenarios, $\xi = 0.3$, $\xi = 0.5$, $\xi = 0.8$, and $\xi = 1$. Figure 5 illustrates the cumulative response of the vaccinated population. As a more cautious observation, this confirms that higher vaccination rates accelerate the accumulation of vaccine-induced protection in the population. In the $\xi = 0.111910$ scenario, the accumulation of the vaccinated population progresses slowly and is only able to reach approximately 1.9×10^8 people by 2023.

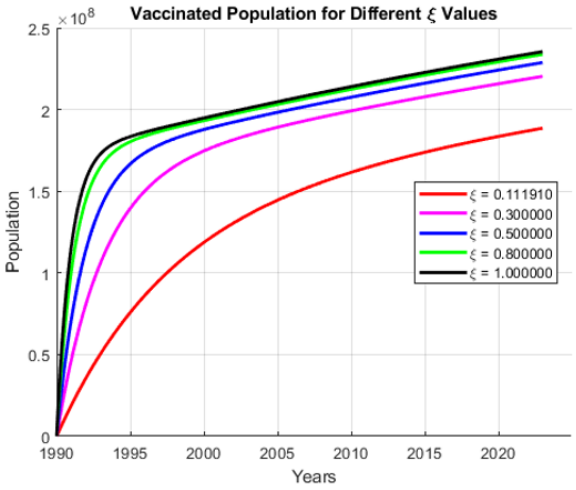

Figure 5. Dynamics of the vaccinated population to the vaccination rate.

As the vaccination rate is increased to the moderate scenarios $\xi = 0.3$ and $\xi = 0.5$, a surge occurs where the protection curve rises sharply and exponentially over the first ten years. When immunization policy is ramped up to the maximum limits of $\xi = 0.8$ and $\xi = 1$, the cumulative curve becomes extremely steep at the start of the simulation period and immediately reaches a steady state above 2.3×10^8 people. This occurs because the susceptible population has been absorbed into compartment V. This experiment provides strong policy recommendations that massive and rapid vaccination interventions at the start of an outbreak are far more effective in containing the spread of meningitis than constant but slow immunization programs.

4. Conclusion

This study developed a six-compartment nonlinear mathematical model (S, E, I, R_s, R_d, V) to analyze meningitis transmission dynamics in Indonesia. Parameter estimation using annual incidence data from 1990–2023 showed close agreement with the observed data, yielding a MAPE of 3.12%. The basic reproduction number was estimated at $\mathcal{R}_0 = 0.1778$, indicating a locally asymptotically stable disease-free equilibrium. Furthermore, sensitivity analysis revealed that the transmission rate (β) and vaccination rate (ξ) are the most influential parameters on changes in $\mathcal{R}_0$ resulting from parameter variation. Numerical simulations demonstrated that a rapid intensification of the mass immunization program at the start of an outbreak is the most effective strategy among the scenarios examined to accelerate vaccine-induced protection and contain the infection.

Despite the insights gained from this modeling approach, several limitations of this study must be acknowledged. First, the parameter estimation relied on a single observed time series of annual meningitis incidence, necessitating the mathematical reconstruction of the remaining compartments due to the absence of direct empirical observations. Second, the model assumes that all parameters remain constant over time, which may not fully capture dynamic changes in population behavior or environmental factors. Furthermore, the empirical data used in this study aggregate various meningitis etiologies—such as bacterial, viral, and fungal—into a single infected compartment, thereby simplifying the distinct transmission characteristics of each pathogen. Finally, the evaluated vaccination interventions serve as hypothetical scenarios and do not incorporate specific operational, logistical, or economic constraints.

Author Contributions. **Aufa Al Musyarof**: Conceptualization, methodology, software, validation, formal analysis, visualization, writing—original draft preparation, writing—review and editing. **Faris Nur Hibban**: Formal analysis, investigation, resources, data curation, writing—original draft preparation. **Mardlijah**: Supervision, validation. **Didik Khusnul Arif**: Project administration, validation.

Acknowledgement. The authors would like to express their gratitude to the Directorate of Research and Community Service, Ministry of Higher Education, Science, and Technology of the Republic of Indonesia, for funding this research under the Regular Fundamental Research Scheme, entitled "*Integrasi Metode Estimasi dan Prediksi Berbasis Extended Kalman Filter dan Long Short Term Memory pada Model Tuberkulosis*". This work was supported under Derivative Contract Agreement Number 2224/PKS/ITS/2026.

Funding. Directorate of Research and Community Service, Ministry of Higher Education, Science, and Technology of the Republic of Indonesia through the Regular Fundamental Research Scheme with Contract Agreement Number 2224/PKS/ITS/2026.

Conflict of interest. There is no conflict of interest regarding the publication of this paper.

Data availability. The meningitis incidence data used in this study are publicly available from the IHME/Our World in Data source cited in Reference [20].

References

[1] World Health Organization, "Meningitis," https://www.who.int/news-room/fact-sheets/detail/meningitis, Apr. 2025, accessed on June 3, 2026.

[2] S. E. Mace, "Acute bacterial meningitis," *Emergency Medicine Clinics of North America*, vol. 26, no. 2, pp. 281–317, 2008, https://doi.org/10.1016/j.emc.2008.02.002.

[3] Centers for Disease Control and Prevention, "About meningitis," https://www.cdc.gov/meningitis/about/index.html, Sep. 2025, accessed on June 3, 2026.

[4] National Institute of Neurological Disorders and Stroke, "Meningitis," https://www.ninds.nih.gov/health-information/disorders/meningitis, 2025, accessed on June 3, 2026.

[5] S. A. Akwetey, A.-H. Osman, F. C. Kotey, A. Awere-Duodu, A. Odoom, B. Opoku-Asare, and E. S. Donkor, "The epidemiology of infectious meningitis in ghana: a systematic review and meta-analysis," *BMC Public Health*, vol. 25, no. 1, p. 2671, 2025, https://doi.org/10.1186/s12889-025-22476-y.

[6] P. P. Agustini, I. M. Subrata, I. G. N. A. S. Pratama, I. D. A. A. A. Shinta, N. P. A. Harjana, S. G. Purnama, R. M. D. Mufa *et al.*, "Design of a streptococcus suis meningitis epidemiological surveillance application to improve zoonotic disease prevention and control in bali province, indonesia," *Journal of Epidemiology and Public Health*, vol. 10, no. 4, pp. 525–538, 2025, https://doi.org/10.26911/jepublichealth.2025.10.04.08.

[7] W. H. Organization *et al.*, "Joint national/international expanded programme on immunization and vaccine preventable disease surveillance review: Indonesia, 10-18 february 2020," https://iris.who.int/items/17ffea67-4a89-4bd5-9ee6-ef5ce509d873, World Health Organization. Regional Office for South-East Asia, Tech. Rep., 2020, accessed on June 3, 2026.

[8] J. K. K. Asamoah, F. Nyabadza, B. Seidu, M. Chand, and H. Dutta, "Mathematical modelling of bacterial meningitis transmission dynamics with control measures," *Computational and mathematical methods in medicine*, vol. 2018, no. 1, p. 2657461, 2018, https://doi.org/10.1155/2018/2657461.

[9] O. Koutou, W. Ouédraogo, H. Ouédraogo, K. Afassinou, and A. B. Diabaté, "Media campaigns, early diagnosis, isolation and treatment on bacterial meningitis outbreak prevention: A modeling study," *Science Progress*, vol. 109, no. 1, p. 00368504251399573, 2026, https://doi.org/10.1177/00368504251399573.

[10] B. Buonomo and R. Della Marca, "A behavioural vaccination model with application to meningitis spread in nigeria," *Applied Mathematical Modelling*, vol. 125, pp. 334–350, 2024, https://doi.org/10.1016/j.apm.2023.09.031.

[11] S. P. Gatyeni, "Mathematical modeling of meningitis transmission dynamics and the impact of vaccination strategies," *Scientific African*, vol. 30, p. e03048, 2025, https://doi.org/10.1016/j.sciaf.2025.e03048.

[12] R. S. br Ginting and Y. A. Adi, "A mathematical model of meningitis with antibiotic effects," *Bulletin of Applied Mathematics and Mathematics Education*, vol. 3, no. 1, pp. 1–14, 2023, https://doi.org/10.12928/bamme.v3i1.9475.

[13] M. I. Amar, M. R. Nisardi, and M. F. Nurahmad, "A deterministic mathematical model of meningitis transmission dynamics with vaccination and screening," *Jurnal Matematika UNAND*, vol. 14, no. 1, pp. 14–30, 2025, https://doi.org/10.25077/jmua.14.1.14-30.2025.

[14] F. Agusto and M. Leite, "Optimal control and cost-effective analysis of the 2017 meningitis outbreak in nigeria," *Infectious Disease Modelling*, vol. 4, pp. 161–187, 2019, https://doi.org/10.1016/j.idm.2019.05.003.

[15] O. J. Peter, A. Yusuf, M. M. Ojo, S. Kumar, N. Kumari, and F. A. Oguntolu, "A mathematical model analysis of meningitis with treatment and vaccination in fractional derivatives," *International Journal of Applied and Computational Mathematics*, vol. 8, no. 3, p. 117, 2022, https://doi.org/10.1007/s40819-022-01317-1.

[16] R. Adawiyah, S. Toaha, and K. Kasbawati, "Stability and bifurcation analysis of mathematical models of meningitis transmission with vaccination and treatment," *Jurnal Matematika, Statistika dan Komputasi*, vol. 18, no. 3, pp. 385–393, 2022, https://doi.org/10.20956/j.v18i3.19714.

[17] C. M. Hazelbag, J. Dushoff, E. M. Dominic, Z. E. Mthombothi, and W. Delva, "Calibration of individual-based models to epidemiological data: A systematic review," *PLoS computational biology*, vol. 16, no. 5, p. e1007893, 2020, https://doi.org/10.1371/journal.pcbi.1007893.

[18] A. H. Amiri Mehra, M. Shafieirad, Z. Abbasi, and I. Zamani, "Parameter estimation and prediction of covid-19 epidemic turning point and ending time of a case study on sir/sqair epidemic models," *Computational and Mathematical Methods in Medicine*, vol. 2020, no. 1, p. 1465923, 2020, https://doi.org/10.1155/2020/1465923.

[19] E. A. Dankwa, L. Cavalli, R. Balasubramanian, M. H. Can, H. Cui, K. M. Jia, Y. Li, S. K. Ofori, N. A. Swartwood, C. G. Wade *et al.*, "Calibration of transmission-dynamic infectious disease models: a scoping review and reporting frame-

work," *PLOS Computational Biology*, vol. 21, no. 11, p. e1013647, 2025, https://doi.org/10.1371/journal.pcbi.1013647.

[20] IHME, Global Burden of Disease, "Incidence of meningitis," https://archive.ourworldindata.org/20260518-095641/grapher/incidence-of-meningitis.html, 2025, accessed on June 3, 2026.

[21] K. Gopal, L. S. Lee, and H.-V. Seow, "Parameter estimation of compartmental epidemiological model using harmony search algorithm and its variants," *Applied Sciences*, vol. 11, no. 3, p. 1138, 2021, https://doi.org/10.3390/app11031138.

[22] N. K.-D. O. Opoku, R. N. Borkor, A. F. Adu, H. N. Nyarko, A. Doughan, E. M. Appiah, B. Yakubu, I. Mensah, and S. P. Salifu, "Modelling the transmission dynamics of meningitis among high and low-risk people in ghana with cost-effectiveness analysis," in *Abstract and Applied Analysis*, vol. 2022, no. 1. Wiley Online Library, 2022, p. 9084283, https://doi.org/10.1155/2022/9084283.

[23] O. J. Peter, F. A. Oguntolu, N. Nyerere, and A. El-Mesady, "Modeling prevalence of meningitis control strategies through evaluating with available data on meningitis cases reported in nigeria," *Modeling Earth Systems and Environment*, vol. 11, no. 4, p. 246, 2025, https://doi.org/10.1007/s40808-025-02417-9.

[24] Badan Pusat Statistik, "Supas 2025: Angka kelahiran total (tfr) sebesar 2,13, angka kematian bayi (imr) sebesar 14,12, dan persentase lansia mencapai 11,97 persen," https://www.bps.go.id/id/pressrelease/2026/05/05/2645/supas-2025--angka-kelahiran-total--tfr--sebesar-2-13---angka-kematian-bayi--imr--sebesar-14-12--dan-persentase-lansia-mencapai-11-97-persen-.html, May 2026, accessed on June 3, 2026.

[25] Kementerian Pendayagunaan Aparatur Negara dan Reformasi Birokrasi, "Data terbaru dukcapil: Penduduk indonesia tembus 288,3 juta jiwa per desember 2025," https://www.menpan.go.id/site/berita-terkini/berita-daerah/data-terbaru-dukcapil-penduduk-indonesia-tembus-288-3-juta-jiwa-per-desember-2025, Mar. 2026, accessed on June 3, 2026.

[26] Kementerian Pendayagunaan Aparatur Negara dan Reformasi Birokrasi , "Ipm indonesia 2025 naik jadi 75,90: Harapan hidup dan pendidikan terus meningkat," https://menpan.go.id/site/berita-terkini/berita-daerah/ipm-indonesia-2025-naik-jadi-75-90-harapan-hidup-dan-pendidikan-terus-meningkat, Nov. 2025, accessed on June 3, 2026.

[27] Badan Pusat Statistik, "Jumlah penduduk hasil sensus penduduk (sp) dan survei penduduk antar sensus (supas) menurut provinsi, 1971 - 2015," https://www.bps.go.id/id/statistics-table/1/MTI2NyMx/jumlah-penduduk--hasil-sensus-penduduk--sp--dan-survei-penduduk-antar-sensus--supas--menurut-provinsi--1971---2015.html, Dec. 2021, accessed on June 3, 2026.

[28] L. Tang, Y. Zhou, L. Wang, S. Purkayastha, L. Zhang, J. He, F. Wang, and P. X.-K. Song, "A review of multi-compartment infectious disease models," *International Statistical Review*, vol. 88, no. 2, pp. 462–513, 2020, https://doi.org/10.1111/insr.12402.